Hyperdeformation in the Cd isotopes: A microscopic analysis

H. Abusara and A. V. Afanasjev
Department of Physics and Astronomy, Mississippi State University, Mississippi 39762, USA
(Received 8 December 2008; revised manuscript received 24 January 2009; published 25 February 2009)

A systematic search for the nuclei in which the observation of discrete hyperdeformed (HD) bands may be feasible with existing detector facilities has been performed in the Cd isotopes within the framework of cranked relativistic mean-field theory. It was found that the ^{96}Cd nucleus is a doubly magic HD nucleus owing to large proton $Z = 48$ and neutron $N = 48$ HD shell gaps. The best candidate for an experimental search of discrete HD bands is the ^{107}Cd nucleus characterized by the large energy gap between the yrast and excited HD bands, the size of which is only 15% smaller than the one in the doubly magic HD ^{96}Cd nucleus.

DOI: 10.1103/PhysRevC.79.024317 PACS number(s): 21.60.Jz, 27.60.+j, 21.10.Ma

I. INTRODUCTION

Hyperdeformation is one of critical phenomena in nuclear structure, the study of which will considerably advance our knowledge of nuclei at extreme conditions of very large deformation and fast rotation [1,2]. Studies of hyperdeformation will also contribute to understanding of the crust of neutron stars, where extremely deformed nuclear structures are expected (see Ref. [3] and references therein). Although there are some experimental evidences of the existence of hyperdeformation at low [4,5] and high spin [6–9], current experimental knowledge of hyperdeformation is very limited. The new generation of detectors such as GRETA [10] and AGATA [11] will definitely allow to study this phenomenon in more detail. However, these detectors will become functional only in the middle of next decade. Thus, it is very important to understand whether new experimental information on hyperdeformation can be obtained with existing detectors such as GAMMASPHERE [12].

Theoretical efforts to study hyperdeformation at high spin both with the macroscopic+microscopic (MM) method and within self-consistent approaches were reviewed in Ref. [1]. Our recent study of hyperdeformation within the framework of the cranked relativistic mean-field (CRMF) theory in the $Z = 40$–58 part of nuclear chart [1] represents the first ever systematic investigation of hyperdeformation within the self-consistent theory. The general features of the hyperdeformed (HD) bands at high spin have been analyzed in Ref. [1]. In particular, it was concluded that the density of the HD states in the vicinity of the yrast line is the major factor that decides whether or not discrete HD bands can be observed. The high density of near-yrast HD states will lead to a situation in which the feeding intensity will be redistributed among many low-lying bands, thus drastically reducing the intensity with which each individual band is populated. For such densities, the feeding intensity of an individual band will most likely drop below the observational limit of the modern experimental facilities. In contrast, the large energy gap between the yrast and excited HD configurations will lead to an increased population of the yrast HD band, thus increasing the chances of its observation.

The analysis of Ref. [1], based on the energy gap between the last occupied and first unoccupied routhians in the yrast HD configurations, suggests that the density of the HD bands in the spin range where they are yrast is high in the majority of the cases. It also indicates the Cd isotopes as the best candidates for a search of discrete HD bands. However, one has to remember that this type of analysis may be too simplistic because the polarization effects induced by particle-hole excitations are neglected. In particular, it can overestimate the size of the energy gap between the yrast and excited HD configurations. Realistic analysis of the density of the HD bands should include significant number of the HD configurations calculated in a fully self-consistent manner with all polarization effects included. Such an analysis is time consuming in a computational sense and has been performed only for ^{124}Xe in Ref. [1], but its extension to other nuclei is needed. Thus, the goals of the current paper are (i) to perform a fully self-consistent analysis of the density of the HD bands in the Cd isotopes and (ii) to find the best nuclei in which experimental study of discrete HD bands can be feasible with existing experimental facilities.

II. THEORETICAL FRAMEWORK AND DETAILS OF THE CALCULATIONS

The calculations are performed in the framework of the CRMF theory without pairing [13,14] using the numerical scheme of Ref. [1]. The CRMF equations for the HD states are solved in the basis of an anisotropic three-dimensional harmonic oscillator in Cartesian coordinates characterized by the deformation parameters $\beta_0 = 1.0$ and $\gamma = 0^\circ$ and oscillator frequency $\hbar\omega_0 = 41A^{-1/3}$ MeV (see Ref. [1] for details). The truncation of the basis is performed in such a way that all states belonging to the shells up to fermionic $N_F = 14$ and bosonic $N_B = 20$ are taken into account; this truncation scheme provides sufficient numerical accuracy [1]. The NL1 parametrization of the relativistic mean-field (RMF) Lagrangian [15] is used in most of our calculations since it provides a good description of the moments of inertia of the rotational bands in the unpaired regime in the superdeformed (SD) and normal-deformed (ND) minima [14,16–18], the single-particle energies for the nuclei around the valley of β stability [16,19], and the excitation energies of the SD minima [20]. Other parametrizations such as NL3 [21], NLSH [22],

NLZ [23], and NL3* [24] are used only to check the size of the HD gaps in the nuclei of interest.

Single-particle orbitals are labeled by $[Nn_z\Lambda]\Omega^{sign}$. $[Nn_z\Lambda]\Omega$ are the asymptotic quantum numbers (Nilsson quantum numbers) of the dominant component of the wave function at $\Omega_x = 0.0$ MeV. The superscripts *sign* to the orbital labels are used sometimes to indicate the sign of the signature r for that orbital ($r = \pm i$).

The excited HD configurations were built from the yrast HD configurations obtained in the previous study [1] by exciting either one proton or one neutron or both together. Proton and neutron configurations generated in this way are labeled by π_i and ν_j, where $i = 0, 1, 2, \ldots$ and $j = 0, 1, 2, \ldots$ are integers indicating the corresponding configurations. $\pi_0 \otimes \nu_0$ represents the yrast HD configuration. Total excited configurations $\pi_i \otimes \nu_j$ are constructed from all possible combinations of proton π_i and neutron ν_j configurations excluding the one with $i = 0$ and $j = 0$. The selection of excited configurations is also constrained by the condition that the energy gap between the orbital from which the particle is excited and the orbital into which it is excited does not exceed 2.5 MeV in the routhian diagram for the yrast HD configuration. All configurations are calculated in a fully self-consistent manner so that their total energies are defined as a function of spin.

Figure 1 illustrates the selection of excited configurations. It shows the occupation of the proton and neutron orbitals in the yrast HD configuration in ^{107}Cd. According to our criteria only three proton excitations across the $Z = 48$ HD gap are considered. In contrast, more neutron particle-hole excitations are allowed across the $N = 59$ HD shell gap. Table I shows their detailed structure. For example, the ν_1 configuration is created by exciting one neutron from the $[770]1/2^+$ into $[413]7/2^+$ orbitals. One can notice that we only consider the particle-hole excitations between the states that do not have the same combination (π, r) of parity π and signature r. The computer code in general can handle the excitations between the states with the same (π, r), but the configurations based on such excitations are less numerically stable and require more computational time. Because of this and the fact that they do not alter significantly the results for the density of the HD states, it was decided to neglect them in the calculations. However, in the cases of large energy gaps between the yrast and excited HD configurations, they are taken into account.

TABLE I. Neutron particle-hole excitations in ^{107}Cd shown in Fig. 1.

Label	Excitation
ν_1	$[770]1/2^+ \rightarrow [413]7/2^+$
ν_2	$[770]1/2^+ \rightarrow [413]7/2^-$
ν_3	$[532]3/2^- \rightarrow [413]7/2^+$
ν_4	$[532]3/2^- \rightarrow [413]7/2^-$
ν_5	$[651]3/2^- \rightarrow [413]7/2^+$
ν_6	$[651]3/2^+ \rightarrow [413]7/2^-$

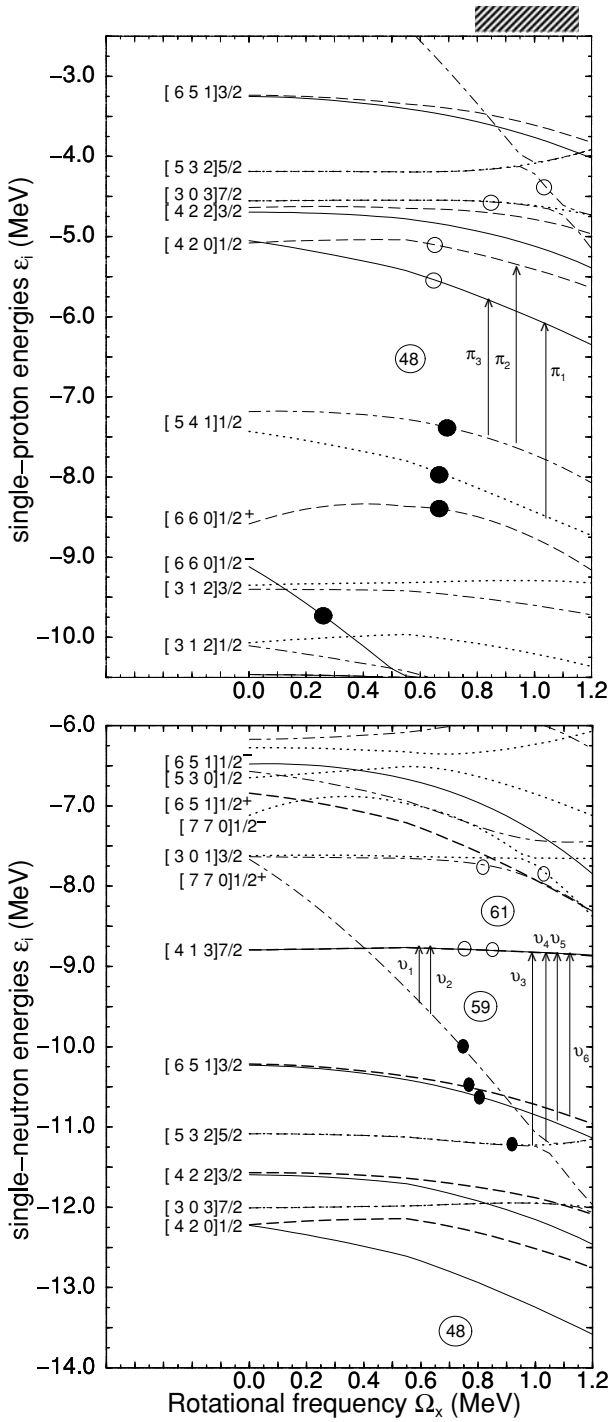

FIG. 1. Proton (top panel) and neutron (bottom panel) single-particle energies (routhians) in the self-consistent rotating potential as a function of the rotational frequency Ω_x. They are given along the deformation path of the yrast HD configuration in ^{107}Cd and obtained in the calculations with the NL1 parametrization of the RMF Lagrangian. Long-dashed, solid, dot-dashed, and dotted lines indicate $(\pi = +, r = +i)$, $(\pi = +, r = -i)$, $(\pi = -, r = +i)$, and $(\pi = -, r = -i)$ orbitals, respectively. Solid (open) circles indicate the orbitals occupied (emptied). The dashed box indicates the frequency range corresponding to the spin range $I = 55\hbar$–$80\hbar$ in this configuration. The arrows indicate the particle-hole excitations leading to excited HD configurations.

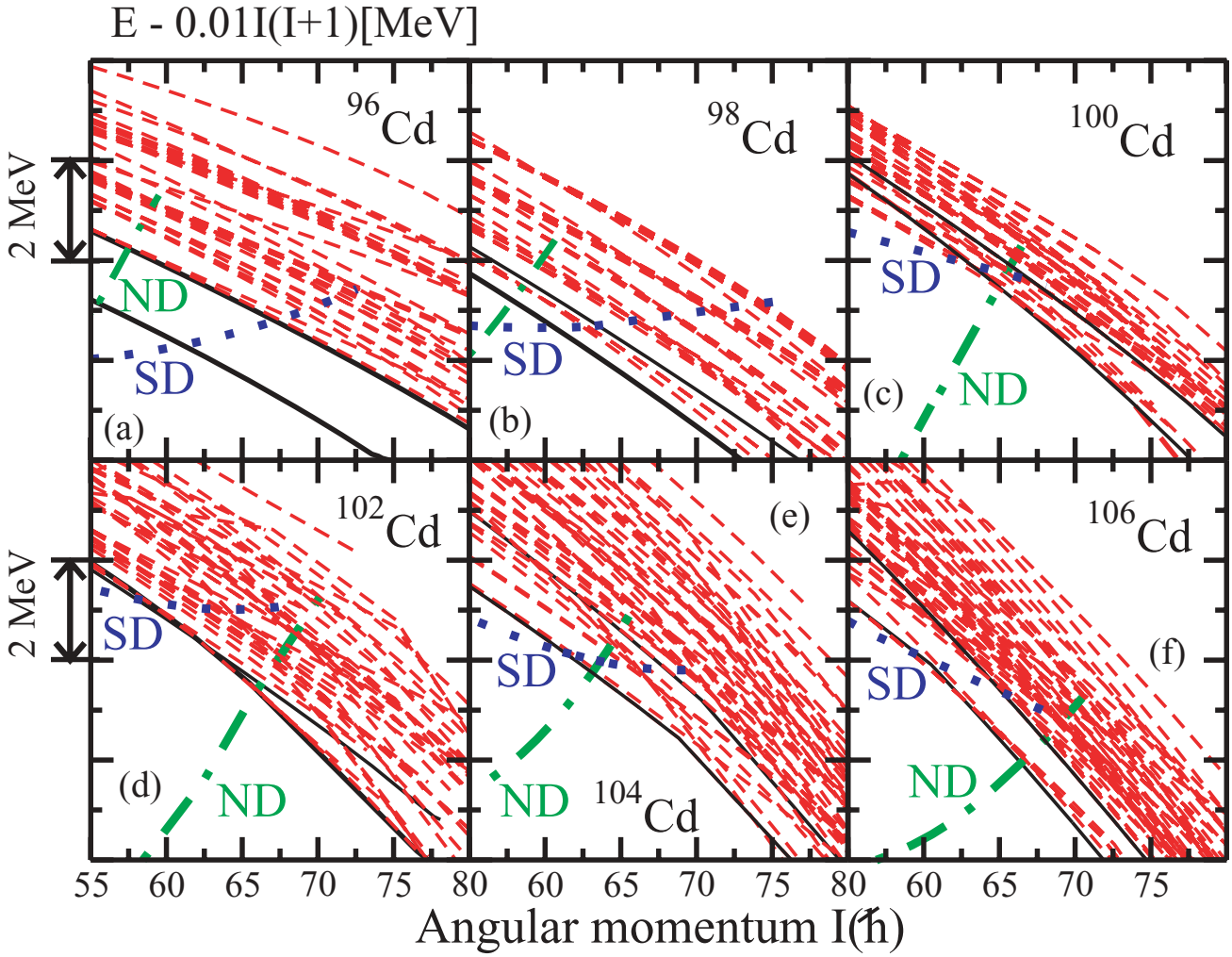

FIG. 2. (Color online) Energies of the calculated HD configurations in even-even $^{96-106}$Cd nuclei relative to a smooth liquid drop reference $AI(I+1)$, with the inertia parameter $A = 0.01$. In each nucleus, the yrast and lowest excited proton configurations are shown by solid lines. Dot-dashed and dotted lines represent the yrast lines at low spin built from normal-deformed (ND) and superdeformed (SD) states, respectively.

III. DISCUSSION

Figures 2 and 3 show the density of the HD states in even-even $^{96-108}$Cd and odd-mass ^{107,109}Cd nuclei studied by using the procedure just outlined. The energy gap between the yrast HD configuration and lowest excited HD configurations is around 1.5 MeV in ^{96}Cd [Fig. 2(a)]. It is comparable with the energy gap between the yrast and excited SD configurations in the doubly magic SD nucleus ^{152}Dy (Fig. 7 in Ref. [14]). This energy gap in ^{96}Cd is due to the large energy cost of particle-hole excitations across the $Z = 48$ and $N = 48$ HD shell gaps, which have similar size (see Fig. 1 and Table II). Taken together this information indicates that ^{96}Cd *is a doubly magic HD nucleus*. Only proton excitations to the $[420]1/2^-$ orbital above the $Z = 48$ HD shell gap result in bound excited proton configurations; the excitations to other orbitals located above the $Z = 48$ HD shell gap produce the proton-emitting states. The doubly magic nature of the ^{96}Cd nucleus is confirmed also in the calculations with other RMF parametrizations (Table II). It is interesting to mention that the RMF parametrizations aimed at the description of the nuclei far from stability such as NL3, NL3*, and NLSH show larger $Z = 48$ and $N = 48$ HD shells gaps in $^{96,107-109}$Cd than the parametrizations NL1 and NLZ fitted predominantly to β-stability nuclei (Table II).

With increasing neutron number the energy gap between the yrast and excited HD configurations disappears (Fig. 2). This is due to the relatively high density of the neutron states above the $N = 48$ HD shell gap (Fig. 1). Indeed, many excited neutron configurations are located below the lowest excited proton configurations (Fig. 2). One can also see that even-even $^{100-104}$Cd nuclei are characterized by appreciable density of the HD states in the vicinity of the yrast HD line (Fig. 2). The analysis of the single-particle structure in these nuclei indicates that similar density of the HD bands is expected also in the odd-mass nuclei $^{99-105}$Cd. In no way can these nuclei to be considered as good candidates for a search of discrete HD bands since the feeding intensity will be redistributed among many low-lying HD bands. As

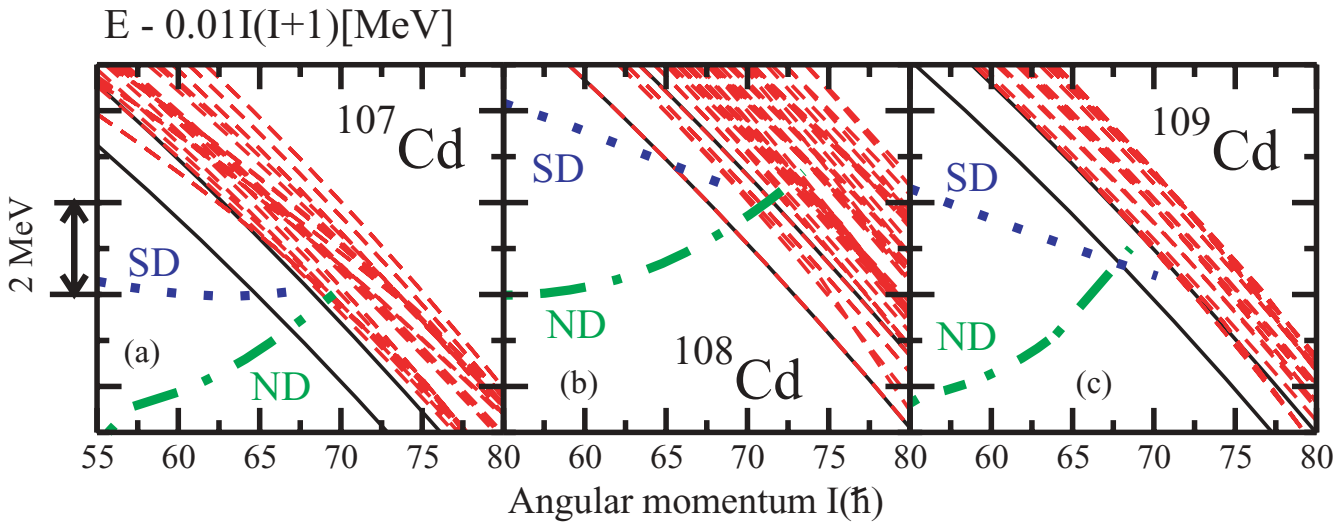

FIG. 3. (Color online) The same as in Fig. 2 but for ^{107,108,109}Cd. The yrast HD line in ^{108}Cd is built from two signature-degenerate configurations.

a result, the feeding intensity of an individual HD band will most likely drop below the observational limit of modern experimental facilities. Although there is some energy gap between the lowest four HD configurations and other excited configurations in ^{106}Cd, this nucleus does not appear to be a good candidate for a search of discrete HD bands because the presence of four low-lying HD configurations will lead to a fragmentation of feeding intensity. This is one possible reason why the HD bands have not been observed in this nucleus [25].

On the other hand, the high density of the HD bands in above discussed nuclei will most likely favor the observation of the rotational patterns in the form of ridge structures in three-dimensional rotational mapped spectra [8]. The study of these patterns as a function of neutron number can provide valuable information about hyperdeformation at high spin.

A further increase of the neutron number brings the neutron Fermi level to the region of low density of the neutron states characterized by the large $N = 59$ and $N = 61$ HD shell gaps (Fig. 1) with the combined size of these two gaps being around 2.5 MeV (Table II). As a result, the $^{107-109}$Cd nuclei show appreciable energy gap between the yrast and lowest excited HD configurations (Fig. 3). This gap is especially pronounced in the case of ^{107}Cd, for which it is around 1.3 MeV. Note that the size of this gap is defined by the size of the $Z = 48$ HD shell gap, since the lowest excited configuration is based on proton excitation [Fig. 3(a)]. Similar or even larger energy gaps between the yrast and excited HD configurations are expected in the NLZ, NL3, NL3*, and NLSH parametrizations for which the size of the $Z = 48$ and $N = 59$ HD shell gaps is at least 1.7 MeV in ^{107}Cd (Table II). The energy gaps between the yrast and excited HD configurations at the spins where the HD configurations become yrast are somewhat lower in ^{108,109}Cd, being around 0.9 and 1.1 MeV. This energy gap in ^{108}Cd is dictated by the size of the $N = 61$ HD shell gap since the lowest excited HD configurations are based on neutron excitations. Thus, in ^{108}Cd it will be smaller in the case of the NLZ parametrization, similar for NL3 and NL3* parametrizations, and larger in the NLSH parametrization as compared with the one obtained in the NL1 parametrization (Table II). In the case of ^{109}Cd, the energy gap between the yrast and excited configurations will be larger in the NL3, NL3*, and NLSH parametrizations and smaller in the NLZ parametrization (Table II).

Two factors make the observation of discrete HD bands in ^{108}Cd[1] with existing facilities less probable than in odd-mass

TABLE II. The size of the $Z = 48$, $N = 59$, and $N = 61$ HD shell gaps (in MeV) obtained with different parametrizations of the RMF Lagrangian for the yrast HD configurations in ^{96,107,108,109}Cd. They are given at rotational frequency $\Omega_x = 1.00$ MeV approximately corresponding to the spin at which the HD bands become yrast. The lowest value (among the different parametrizations) of the shell gap is shown in bold. The "59 + 61" line shows the combined size of the $N = 59$ and $N = 61$ HD shell gaps.

Nucleus	RMF parametrizations					
	Gap	NL1	NLZ	NL3	NL3*	NLSH
^{96}Cd	$Z = 48$	**1.75**	1.93	2.43	2.27	2.71
	$N = 48$	**2.00**	2.07	2.59	2.44	3.03
^{108}Cd	$Z = 48$	**1.62**	1.66	2.23	1.99	2.06
	$N = 59$	1.30	1.70	1.50	1.46	**1.20**
	$N = 61$	1.20	**0.74**	1.20	1.19	1.50
	59 + 61	2.50	**2.44**	2.70	2.65	2.70
^{107}Cd	$Z = 48$	**1.70**	1.73	2.22	2.18	2.27
	$N = 59$	1.89	2.16	2.08	2.04	**1.74**
^{109}Cd	$Z = 48$	**1.52**	1.61	1.89	1.84	1.54
	$N = 61$	1.37	**1.16**	1.83	1.74	2.16

[1]Two bands with very extended shapes observed in ^{108}Cd in Refs. [26,27] were assigned as superdeformed in Ref. [28].

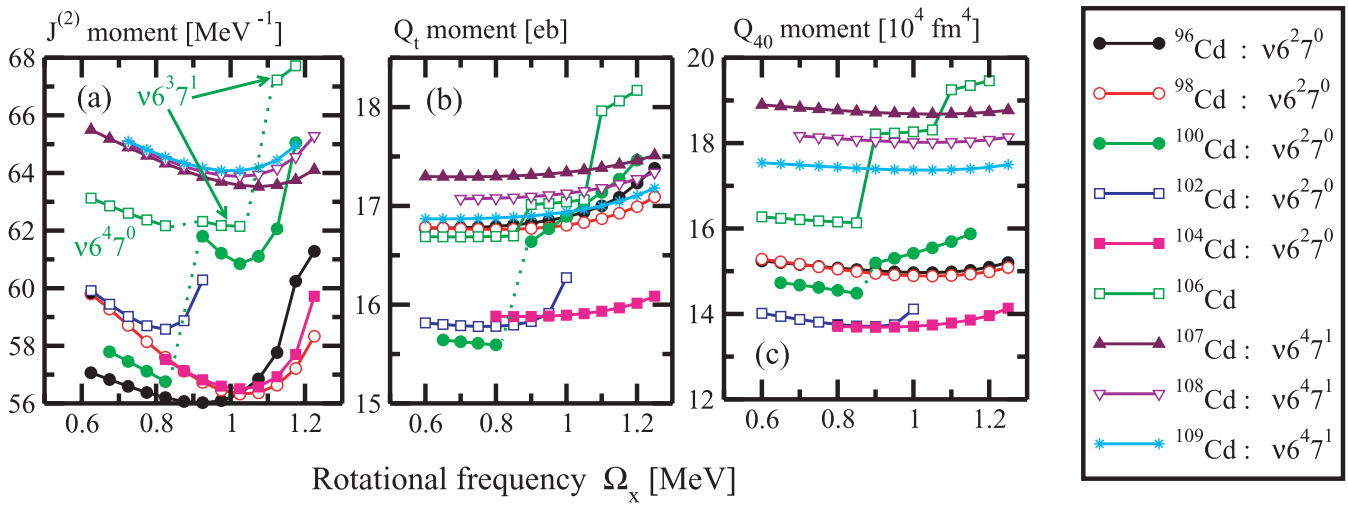

FIG. 4. (Color online) Dynamic moments of inertia $J^{(2)}$ (a), transition quadrupole moments (b), and mass hexadecapole moments Q_{40} (c) of the yrast HD bands in the nuclei under study. All these bands have the proton $\pi 6^2$ configuration; their neutron configurations are shown in the right panel. The configuration of the yrast HD band in ^{106}Cd is shown in panel (a).

^{107,109}Cd nuclei. First, the yrast HD line in this nucleus is built from two signature-degenerate configurations [Fig. 3(b)] in which the last neutron is placed into one of the signatures of the [413]7/2 orbital (see Fig. 1 and Ref. [28]). This reduces the feeding intensity of each of these bands by factor of 2 as compared with the case when the yrast HD line is built from a single configuration. Second, the energy gap between the yrast and excited HD configurations decreases with increasing spin [Fig. 2(b)]. As a result, further reduction of feeding intensity of the yrast HD bands is expected if the bands are populated at spins higher than the spin at which they become yrast. In contrast, the energy gap between the yrast and excited HD configurations is more constant as a function of spin in ^{109}Cd and especially in ^{107}Cd. *All these results strongly suggest that the* ^{107}Cd *nucleus is the best candidate for the experimental search of the discrete HD bands*. This conclusion is also supported by detailed analysis of the single-particle routhians in the yrast HD configurations of even-even nuclei studied in Ref. [1]; this analysis does not suggest any alternative case that would provide similar or larger gap between the yrast and excited HD configurations in even-even, odd, and odd-odd nuclei of the $Z = 40$–58 part of the nuclear chart.

The calculated properties of the yrast HD bands in the studied nuclei are shown in Fig. 4. The HD shapes undergo a centrifugal stretching that results in an increase of the transition quadrupole moments Q_t with increasing rotational frequency. This process also reveals itself in the dynamic moments of inertia, which increase with increasing rotational frequency in the frequency range of interest. However, the mass hexadecapole moments Q_{40} do not show a clear trend as a function of rotational frequency and stay nearly constant in the majority of the HD bands. Unpaired band crossings resulting from the interaction of different single-particle orbitals are seen in the configurations of the yrast HD bands in ^{100,102,106}Cd nuclei. For example, the interaction between the $(r = +i)$ signatures of the $\nu[770]1/2$ and $\nu[532]5/2$ orbitals is responsible for the crossing seen at $\Omega_x \sim 1.05$ MeV in the yrast HD band in ^{106}Cd. This crossing may be an extra factor (in addition to the density of the near-yrast HD bands) that complicates the observation of the HD bands in ^{106}Cd: Such bands have not been observed in the experiment of Ref. [25].

The current study clearly shows that the polarization effects in time-even and time-odd mean fields have an important impact on the density of the HD states and especially on the energy gap between the yrast and excited HD states. The latter quantity is appreciably smaller (by up to ~ 0.5 MeV; compare Figs. 2 and 3 with Table II) than the respective HD shell gap in the routhian diagram.

The role of time-odd mean fields in the definition of the energy gap between the yrast and excited HD configurations is quite complicated. This is illustrated by the fact that the energy gap between the yrast HD and the lowest excited proton and neutron HD configurations is larger by $\approx$0.2 MeV in the calculations without nuclear magnetism (NM) [29] than in the ones with NM at spins where the HD configurations become yrast ($I \approx 67\hbar$). This fact reflects two different mechanisms by which the time-odd mean fields affect the relative energies of different rotational bands. In the first mechanism, the angular momentum content of the single-particle orbitals is modified in the presence of time-odd mean fields (see Ref. [29] for details). There are two important consequences of this mechanism. First, the same total angular momentum of the system is built at a rotational frequency that is $\sim$25% lower in the calculations with NM than in the calculations without NM. Second, the changes of the single-particle angular momenta of the single-particle orbitals surrounding the HD gaps of interest (the $\pi[420]1/2$ and $\pi[541]1/2$ orbitals for the proton subsystem and the $\nu[413]7/2$ and $\nu[651]3/2$ orbitals for the neutron subsystem; Fig. 1) induced by NM modify the single-particle energies of these orbitals. As a result, these gaps are smaller by $\sim$0.12 MeV in the calculations with NM at $I = 67\hbar$. The second mechanism

is related to additional binding due to time-odd mean fields. The time-odd mean fields are stronger in the excited HD configuration than in the yrast HD configuration. Thus, additional binding due to NM is stronger in the excited HD configuration than in the yrast HD configuration. This also leads to the decrease of the energy gap between the yrast and excited HD configurations in the calculations with NM as compared with the ones without NM.

The presence of time-odd mean fields reveals itself also in the energy splitting of the opposite signatures of the $\nu[770]1/2$ orbital visible at $\Omega_x = 0.0$ MeV (Fig. 1); the occupied orbital is more bound than the unoccupied one in the RMF theory [14].

When considering theoretical predictions one has to keep in mind that they are subject to errors in the description of the energies of the single-particle states, which exist in the RMF theory at spherical shape [30], normal deformation [19], and quite likely at superdeformation [28]. The extrapolation from spherical and normal deformation toward hyperdeformation is itself a potential source of errors since it is not know how well the response of the mean field (or the single-particle potential and liquid drop in the MM method) to the extreme elongation of the nucleus is reproduced in model calculations. Such errors are not restricted to self-consistent models; they are also expected in the phenomenological potentials (used in the MM method) that describe single-particle energies at normal deformation better than self-consistent models. However, several facts support the results and interpretations given here. First, all RMF parametrizations used in this study lead to the same HD configurations in $^{96,107-109}$Cd nuclei that become yrast at similar spins (see Ref. [1] for comparison of the results obtained with NL1 and NL3) and to similar sizes of the proton and neutron HD shell gaps (Table II). Second, the large size of the $Z = 48$ and $N = 59$ (and especially of the combined neutron $59 + 61$) HD shell gaps reduces the importance of the errors in the description of the energies of specific single-particle states. Third, the MM results of Ref. [31] suggest similar conclusions for the nuclei around ^{108}Cd. Indeed, a large $Z = 48$ shell gap and a low density of the single-particle states in the vicinity of the $N = 59$ and $N = 61$ HD shell gaps is clearly visible in Figs. 4 and 5 of Ref. [31]. The $N = 59$ and $N = 61$ shell gaps are separated by the signature-degenerate $7/2^+$ state (Fig. 5 in Ref. [31]). Thus, similar to our case, the yrast HD line in ^{108}Cd will be formed from two signature-degenerate configurations in the MM calculations.

IV. CONCLUSIONS

In summary, a systematic analysis of hyperdeformation in the Cd isotopes has been performed in the cranked relativistic mean-field theory. The density of the HD states has been analyzed with the goal of finding the best cases for experimental search of the discrete HD bands. Our analysis indicates ^{96}Cd as a doubly magic HD nucleus in this part of the nuclear chart; its magicity is due to large $Z = 48$ and $N = 48$ HD shell gaps. However, experimental study of hyperdeformation in this nucleus is problematic with existing facilities owing to its $N = Z$ status. The low density of the neutron single-particle states in the vicinity of the $N = 59$ and 61 HD shell gaps and sizable $Z = 48$ HD shell gap lead to appreciable gaps between the yrast and excited HD bands in $^{107-109}$Cd nuclei, thus offering better opportunities to observe discrete HD bands. Among these three nuclei, the best candidate for observing the discrete HD bands with existing facilities is the ^{107}Cd nucleus. The MM calculations of Refs. [31,32] indicate that the fission barriers are sufficiently large in the nuclei around ^{108}Cd so that the HD minimum could survive fission for a significant range of angular momentum. The stability of the HD minimum is defined by its depth, the fission barrier height, and the height of the barrier between the HD and normal-deformed/superdeformed minima [2,32]. Our study clearly indicates that the HD minimum is localized in the potential energy surface. However, future studies of hyperdeformation in this mass region have to provide more quantitative answers for these properties of the HD minima in a fully self-consistent framework.

ACKNOWLEDGMENT

The work was supported by the US Department of Energy under Grant No. DE-FG02-07ER41459.

[1] A. V. Afanasjev and H. Abusara, Phys. Rev. C **78**, 014315 (2008).
[2] J. Dudek, K. Pomorski, N. Schunck, and N. Dubray, Eur. Phys. J. A **20**, 15 (2004).
[3] N. Chamel, Nucl. Phys. **A747**, 109 (2005).
[4] A. Krasznahorkay, M. Hunyadi, M. N. Harakeh, M. Csatlós, T. Faestermann, A. Gollwitzer, G. Graw, J. Gulyás, D. Habs, R. Hertenberger, H. J. Maier, Z. Máté, D. Rudolph, P. Thirolf, J. Timár, and B. D. Valnion, Phys. Rev. Lett. **80**, 2073 (1998).
[5] C. M. Brink, H. Friedrich, A. Weiguny, and C. W. Wong, Phys. Lett. **B33**, 143 (1970).
[6] A. Galindo-Uribarri, H. R. Andrews, G. C. Ball, T. E. Drake, V. P. Janzen, J. A. Kuehner, S. M. Mullins, L. Persson, D. Prévost, D. C. Radford, J. C. Waddington, D. Ward, and R. Wyss, Phys. Rev. Lett. **71**, 231 (1993).
[7] G. Viesti, M. Lunardon, D. Bazzacco, R. Burch, D. Fabris, S. Lunardi, N. H. Medina, G. Nebbia, C. Rossi-Alvarez, G. de Angelis, M. De Poli, E. Fioretto, G. Prete, J. Rico, P. Spolaore, G. Vedovato, A. Brondi, G. La Rana, R. Moro, and E. Vardaci, Phys. Rev. C **51**, 2385 (1995).
[8] B. Herskind, G. B. Hagemann, G. Sletten, Th. Døssing, C. Rønn Hansen, N. Schunck, S. Ødegård, H. Hübel, P. Bringel, A. Bürger, A. Neusser, A. K. Singh, A. Al-Khatib, S. B. Patel, A. Bracco, S. Leoni, F. Camera, G. Benzoni, P. Mason, A. Paleni, B. Million, O. Wieland, P. Bednarczyk, F. Azaiez, Th. Byrski, D. Curien, O. Dakov, G. Duchene, F. Khalfallah, B. Gall, L. Piqeras, J. Robin, J. Dudek, N. Rowley, B. M. Nyakó, A. Algora, Z. Dombradi, J. Gal, G. Kalinka, D. Sohler, J. Molnár, J. Timár, L. Zolnai, K. Juhász, N. Redon, F. Hannachi, J. N. Scheurer, J. N. Wilson, A. Lopez-Martens, A. Korichi, K. Hauschild, J. Roccaz, S. Siem, P. Fallon, I. Y. Lee, A. Görgen, A. Maj, M. Kmiecik, M. Brekiesz, J. Styczen, K. Zuber, J. C. Lisle, B. Cederwall, K. Lagergren, A. O. Evans, G. Rainovski,

G. De Angelis, G. La Rana, R. Moro, W. Gast, R. M. Lieder, E. Podsvirova, H. Jäger, C. M. Petrache, and D. Petrache, Phys. Scr. T **125**, 108 (2006).
[9] W. von Oertzen, V. Zherebchevsky, B. Gebauer, Ch. Schulz, S. Thummerer, D. Kamanin, G. Royer, and Th. Wilpert, Phys. Rev. C **78**, 044615 (2008).
[10] I.-Y. Lee, AIP Conf. Proc. **656**, 343 (2003).
[11] D. Bazzacco, AIP Conf. Proc. **701**, 265 (2004).
[12] I.-Y. Lee, Nucl. Phys. **A520**, 641c (1990).
[13] W. Koepf and P. Ring, Nucl. Phys. **A493**, 61 (1989).
[14] A. V. Afanasjev, J. König, and P. Ring, Nucl. Phys. **A608**, 107 (1996).
[15] P.-G. Reinhard, M. Rufa, J. Maruhn, W. Greiner, and J. Friedrich, Z. Phys. A **323**, 13 (1986).
[16] A. V. Afanasjev, G. Lalazissis, and P. Ring, Nucl. Phys. **A634**, 395 (1998).
[17] A. V. Afanasjev, I. Ragnarsson, and P. Ring, Phys. Rev. C **59**, 3166 (1999).
[18] D. Vretenar, A. V. Afanasjev, G. Lalazissis, and P. Ring, Phys. Rep. **409**, 101 (2005).
[19] A. V. Afanasjev, T. L. Khoo, S. Frauendorf, G. A. Lalazissis, and I. Ahmad, Phys. Rev. C **67**, 024309 (2003).
[20] G. A. Lalazissis and P. Ring, Phys. Lett. **B427**, 225 (1998).
[21] G. A. Lalazissis, J. König, and P. Ring, Phys. Rev. C **55**, 540 (1997).
[22] M. M. Sharma, M. A. Nagarajan, and P. Ring, Phys. Lett. **B312**, 377 (1993).
[23] M. Rufa, P.-G. Reinhard, J. A. Maruhn, W. Greiner, and M. R. Strayer, Phys. Rev. C **38**, 390 (1988).
[24] G. A. Lalazissis, S. Karatzikos, R. Fossion, D. Pena Arteaga, A. V. Afanasjev, and P. Ring, Phys. Lett. **B671**, 36 (2009).
[25] P. Fallon, Nucl. Phys. **A752**, 231c (2005).
[26] R. M. Clark, P. Fallon, A. Görgen, M. Cromaz, M. A. Deleplanque, R. M. Diamond, G. J. Lane, I. Y. Lee, A. O. Macchiavelli, R. G. Ramos, F. S. Stephens, C. E. Svensson, K. Vetter, D. Ward, M. P. Carpenter, R. V. F. Janssens, and R. Wadsworth, Phys. Rev. Lett. **87**, 202502 (2001).
[27] A. Görgen, R. M. Clark, P. Fallon, M. Cromaz, M. A. Deleplanque, R. M. Diamond, G. J. Lane, I. Y. Lee, A. O. Macchiavelli, R. G. Ramos, F. S. Stephens, C. E. Svensson, K. Vetter, D. Ward, M. P. Carpenter, R. V. F. Janssens, and R. Wadsworth, Phys. Rev. C **65**, 027302 (2002).
[28] A. V. Afanasjev and S. Frauendorf, Phys. Rev. C **72**, 031301(R) (2005).
[29] A. V. Afanasjev and P. Ring, Phys. Rev. C **62**, 031302(R) (2000).
[30] K. Rutz, M. Bender, P.-G. Reinhard, J. A. Maruhn, and W. Greiner, Nucl. Phys. **A634**, 67 (1998).
[31] R. R. Chasman, Phys. Rev. C **64**, 024311 (2001).
[32] N. Schunck, J. Dudek, and B. Herskind, Phys. Rev. C **75**, 054304 (2007).